THEORETICA CHIMICA ACTA

Theoret. Chim. Acta (Berl.) 60, 523–533 (1982)

Dynamic Behavior of the IRC in Chemical Laser Systems

Koichi Yamashita, Tokio Yamabe, and Kenichi Fukui

Department of Hydrocarbon Chemistry, Faculty of Engineering, Kyoto University, Kyoto, Japan

The *ab initio* potential energy surface of the HF elimination reaction of CH_2FOH is surveyed. In order to elucidate the mechanism of the vibrational excitation of the product HF, the "vibrational frequency correlation diagram" is analyzed along the IRC.

Key words: Intrinsic reaction coordinate – Chemical laser system – Vibrational frequency correlation diagram.

1. Introduction

Recently, there has been much experimental [1] and theoretical [2] interest in the reactions of electronically excited oxygen atoms with organic molecules. The systems, known in combustion and atmospheric chemistry, are rather important in the discovery of new chemical laser systems.

Chemical HF laser emissions arising from the reactions of ^3P and ^1D oxygen atoms with fluorides have been reported recently by Lin et al. [3, 4]. The vibrationally excited HF was proposed to be resulting from the insertion–elimination sequence of reactions. They interpreted that the excited intermediate is short-lived and thus the total available reaction energy has not been randomized effectively before the dissociation takes place.

The production of vibrationally excited products is caused by chemical activation as in the case of oxygen atom reactions, as well as by physical activation, such as photoexcitation [5]. The condition essential to laser action is the selective population of product vibrational states which provides the population inversion.

The observed dynamics would be ultimately correlated to the main features of potential surface, such as the geometries of critical points and the vibrational

0040-5744/82/0060/0523/$02.20

motions along a reaction path. It is therefore the first step to examine the qualitative surface features which are responsible for important dynamical effects [6].

In this paper, the *ab initio* potential energy surface of the HF elimination reaction of CH_2FOH is carefully examined in terms of the intrinsic reaction coordinate (IRC) by Fukui [7]. The transition state of the reaction is located on the multi-dimensional potential surface and starting from the saddle point by tracing the IRC to the reactant complex as well as to the product, the dynamical aspects of the system are investigated. The theoretical tracing of IRC gives us the very motion of the atoms which construct the chemically reacting system and makes possible to analyze the vibrational motions perpendicular to IRC [8–10]. This gives a dynamical picture in a local system around the reaction path. Using the optimized geometries and calculated vibrational frequencies, RRKM calculations [11] are performed to estimate the lifetime of the reactant complex.

2. Results and Discussion

2.1. Potential Energy Surface of the System

It is well accepted that certain dominant features of the potential energy surface govern the chemical reactivity and its dynamics. The critical points on the reaction path, in particular, play the central role. A knowledge of the transition state, which can hardly be detected experimentally, is available from theoretical studies.

The reactant complex CH_2FOH, the elimination products HF, H_2CO as well as the transition state connecting them are searched by the energy gradient method [12] with the 4-31G basis set [13]. The four-centered transition state with C_s symmetry is obtained as shown in Fig. 1(a). The HF elimination reaction was predicted to proceed most effectively this type of four-centered transition state [4]. By vibrational analysis the transition state is identified as the saddle point on the potential energy surface. The arrows in the figure indicate the displacement vectors of the normal mode with an imaginary frequency which gives an initial direction of the IRC. They involve the concerted formation of the C=O and HF bonds and cleavage of the CF and OH bonds. The IRC starting from the transition state in the direction of the vector and in the reverse direction successfully approaches the product and the reactant complex, respectively. The detailed analysis of the vibrational modes at the transition state and of the IRC are discussed in later sections.

Compared with the reactant complex geometry in Fig. 1(b) and the product, the CO bond length is intermediate between those of the reactant and the product H_2CO (1.206 Å). The CF and OH bond lengths are stretched by 33 and 26%, respectively. The H_2CO segment is fairly similar to that of the product H_2CO (HCH = 116.4°, CH = 1.080 Å). It is noted that the HF bond distance is longer than that of the product HF (0.923 Å) by 33%. The analogous four-centered transition state of the HF elimination from CH_3CH_2F by Kato and Morokuma [14] on the same level of calculations has a similar HF distance (1.281 Å). A

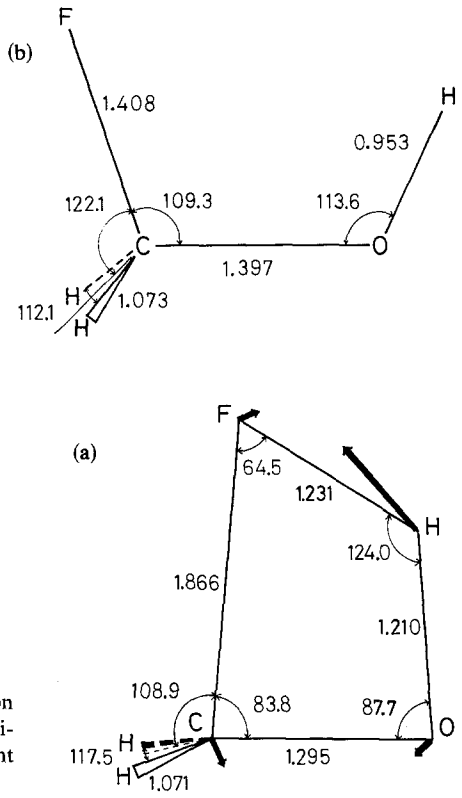

Fig. 1. Optimized geometries of **(a)** the transition state and **(b)** the reactant complex for the HF elimination. The arrows are the initial displacement vectors of IRC

significant geometrical difference going from the transition state to the product is correlated to the vibrational excitation of the HF stretching mode as suggested by them [14].

The exothermic energy is 39.4 kcal/mol and the threshold energy is estimated to be 57.7 kcal/mol on the 4-31G SCF level. In order to improve the potential barrier, configuration interaction calculations [15] are carried out using the optimized geometries. All singly and doubly excited configurations, about 20 000, are included. The unlinked quadruple excitation contribution was estimated using Davidson's formula [16]. The calculated relative energies with the zero-point-energy correction estimated from the calculated vibrational frequencies are listed in Table 1. The vibrational modes at the reactant complex are analyzed in the next section. The best calculated barrier, on the (S+D)CI+QC level, is obtained to be 44.2 kcal/mol and the exothermic energy is 42.5 kcal/mol. Although experimental values are not available to our knowledge, the relative energies are estimated with an accuracy of 2–3 kcal/mol on this level of calculations [14]. The calculated best barrier is used in the RRKM calculations. Examining the contribution of the SCF reference configuration, the potential surface of the HF elimination reaction is qualitatively well described within the SCF calculation (CH_2FOH: 0.957, transition state: 0.952, H_2CO: 0.960, HF: 0.985).

Table 1. Total (E_T; in Hartree) and relative (ΔE; in kcal/mol) energies for CH_2FOH, transition state, and $H_2CO + HF$

	SCF		(S+D)CI		(S+D)CI+QC[b]	
	E_T	ΔE[a]	E_T	ΔE[a]	E_T	ΔE[a]
CH_2FOH	−213.6091	0	−213.9282	0	−213.9551	0
transition state	−213.5171	53.3	−213.8466	46.8	−213.8776	44.2
$H_2CO + HF$	−213.5799	12.9	−213.9232	−2.3	−213.9438	1.7

[a] The zero-point correction is included. The zero-point energies are 29.5, 25.2, and 24.2 kcal/mol for CH_2FOH, transition state, and $H_2CO + HF$, respectively.
[b] Unlinked cluster quadruples correction.

2.2. Vibrational Analyses of the Reactant Complex and Transition State

Since the vibrational frequencies and their assignments for CH_2FOH and of course at the transition state are not available in literature, Lin et al. in their RRKM calculations used the frequencies composed of the known assignment of the related compounds CH_3F and CH_3OH [4]. In this section, we perform the vibrational analyses at these points.

The calculated normal modes and their frequencies at the reactant complex and the transition state are given in Table 2. The second derivatives of the potential energy required for the vibrational analysis are obtained by numerical differentiations of the analytically calculated energy gradient [17]. It is well accepted that the ordering of vibrational frequencies is well reproduced on our level of calculations and that the experimental frequencies would be obtained by a reduction of 10–15% from the calculated ones [17]. It is noted that the OCF bending mode of the reactant complex is the weakest, which would play an important part in the elimination due to its mechanism of complex formation. Schematic representations of the displacement vectors of the normal modes at the transition state are given in Fig. 2. The imaginary frequency at the transition state is calculated to be 2038i, indicating that the saddle point region is a steep cliff. The property of the normal mode is the combination of the HF and C=O stretching modes and the translational motion between the departing segments as seen previously.

2.3. Analysis of IRC

The tracing of IRC gives a set of atomic coordinates as a function of s, the length measured along the IRC, for the initial direction of steepest descent at the transition state and the infinitesimal kinetic energy. This procedure may be used then to illustrate the progress of reaction; the changes of displacement vectors of IRC which give the direction of the instantaneous atomic motion regarding the reaction dynamics. The analysis of the dynamic aspects of some physical properties along IRC, the central line of reaction trajectory is called "reaction ergodography" [18]. For example, Fig. 3 is a profile along the IRC for HF elimination.

Table 2. a. Calculated normal modes and their frequencies of CH_2FOH

mode		approximate assignment	frequency (cm^{-1})
A′	ν_1	OH stretching	3974
	ν_2	CH stretching	3308
	ν_3	CH_2 scissor	1717
	ν_4	CH_2F deformation	1594
	ν_5	OH bending	1378
	ν_6	CO stretching	1164
	ν_7	CF stretching	1034
	ν_8	OCF bending	505
A″	ν_9	CH stretching	3380
	ν_{10}	CH_2F deformation	1369
	ν_{11}	CH_2F rocking	1239
	ν_{12}	torsion[a]	391i

[a] Since we consider the eclipsed CH_2FOH, the frequency of torsion is obtained to be imaginary. The mode is excluded in the RRKM calculations.

Table 2. b. Calculated normal modes and their frequencies of transition state

mode		approximate assignment	frequency (cm^{-1})
A′	ν_1	CH stretching	3330
	ν_2	HF + OH stretching	2112
	ν_3	Reaction coordinate	2038i
	ν_4	CH_2 scissor	1726
	ν_5	CO stretching	1419
	ν_6	CH_2 wagging	1382
	ν_7	OCF bending	719
	ν_8	CF stretching	514
A″	ν_9	CH stretching	3447
	ν_{10}	CH_2 rocking	1303
	ν_{11}	HF + H_2CO rotation	1043
	ν_{12}	torsion	594

The displacement vectors of IRC are schematically given in Fig. 4 for each value of s. In the early stage of reaction, $s = -1.8$, the displacement vector is composed of that of the CF stretching as well as that of the OCF bending modes. Then, near the transition state, $s = -0.6$, the component of the OH bending mode becomes significant. After the transition state, the displacement vector reveals the relative motion between the products HF and H_2CO. The component of the HF stretching mode already disappears at $s = 0.5$. Kato and Morokuma's calculations [14] on the curvature of IRC suggested that the energy disposal into the HF stretching

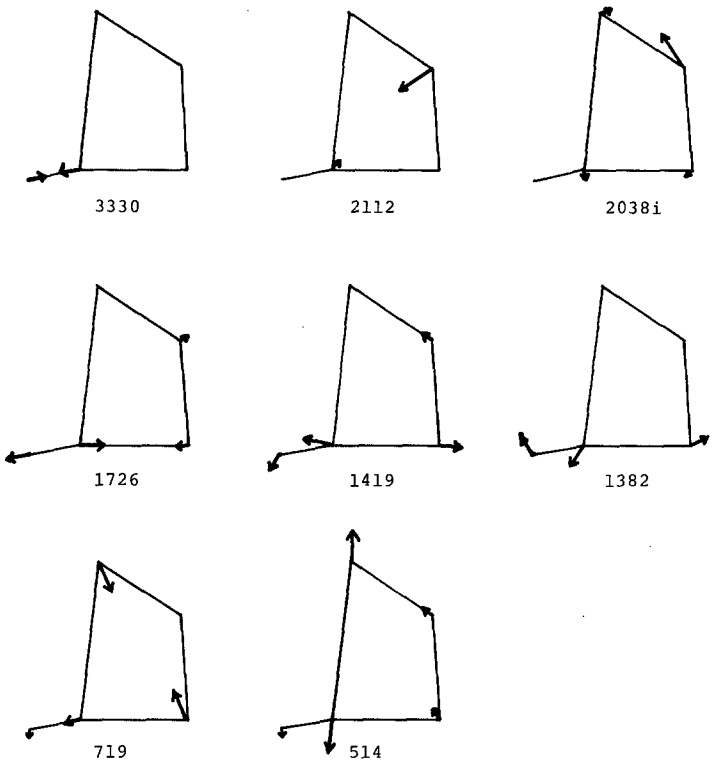

Fig. 2. Schematic representation of the normal modes at the transition state

vibrations occurs in the region where its contribution in the IRC components drastically decreases. The rapid change of the HF stretching component in our system will also be correlated to the twisting of the IRC. The location of the IRC twisting in configuration space can be investigated by "vibrational frequency correlation diagram" [10]. The procedure is performed in a later section.

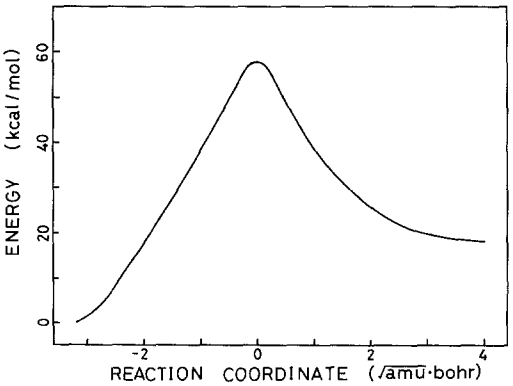

Fig. 3. Potential profile along the IRC

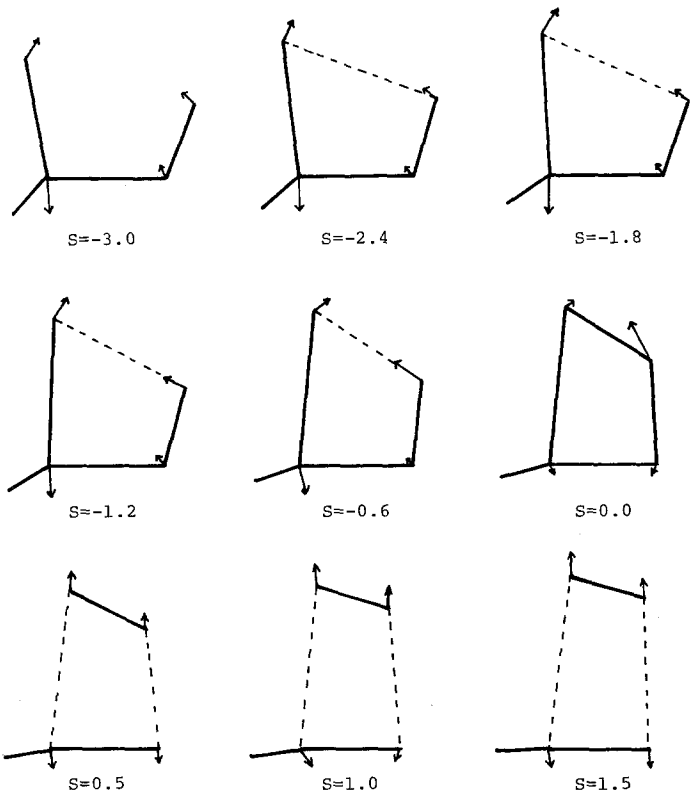

Fig. 4. Changes of the displacement vector of the IRC. The transition state is located at $s = 0.0$

2.4. Lifetime of the Reactant Complex

There are two extreme modes of reactive collisions depending on the lifetime of its transient complex; the direct and complex modes. In case of the system with which we concern, the energy of the newly-formed bond by collision between the oxygen atom and CH_2F is available as excitation energy of the newly-formed molecules, which will either ultimately dissociate by HF elimination or, in the presence of other molecules, stabilize by energy transfer collisions.

At higher translational energies, in the case of a direct mode, eventually it is energetically unnecessary that the system exits along the product valley. The mechanism of formation of the reactant complex as well as the characteristics of the potential surface leading to the transition state will govern the reaction dynamics.

On the other hand, over the long lifetime of the reactant complex there is ample time for energy exchange between the different vibrational modes and hence all memory of the initial conditions is erased. Therefore, the dynamics of the reaction will be determined by the potential surface features in the course from the transition state to the products.

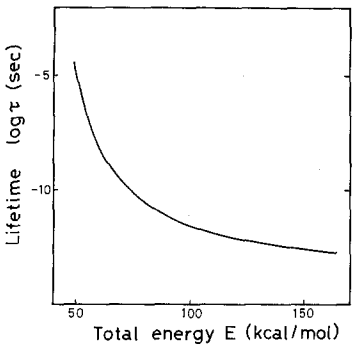

Fig. 5. RRKM lifetime of the reactant complex

In this section, we estimate the lifetime of the reactant complex in various energy ranges. Fig. 5 shows the lifetime of the reactant complex as a function of total energy. The lifetime was obtained as the reciprocal of the RRKM reaction rate assuming the elimination path is the only decay process. The RRKM calculations were performed using the calculated frequencies and the moments of inertia in Table 3, where the overall rotations are regarded as adiabatic. The available energy produced by the insertion of the oxygen atom was estimated experimentally to be about 140 kcal/mol [4]. In this energy, the lifetime is shorter than 10^{-12} sec, similar to a lifetime of the typical vibrational period of direct-mode reactions. Near threshold energy, the reaction complex has a long lifetime, 10^{-5} sec. Therefore, whether an energy randomization occurs or not determines the mechanism of intramolecular energy transfer of the system. A knowledge of the nature of the potential surface from the complex region to the products would be useful.

2.5. Vibrational Coupling Along the IRC

In this section, the vibrational motions perpendicular to the IRC are analyzed in order to investigate the dynamical coupling between the normal modes as well as the normal modes and the IRC.

Figure 6 is the "vibrational frequency correlation diagram" which correlates the vibrational frequencies of the reactant with those of the product, through those of the transition state [10]. The frequencies of the normal modes were calculated by

Table 3. Moments of inertia (amuÅ^2) for CH_2FOH and transition state

	CH_2FOH	Transition state
I_A	56.66	58.24
I_B	48.20	45.56
I_C	11.66	16.06

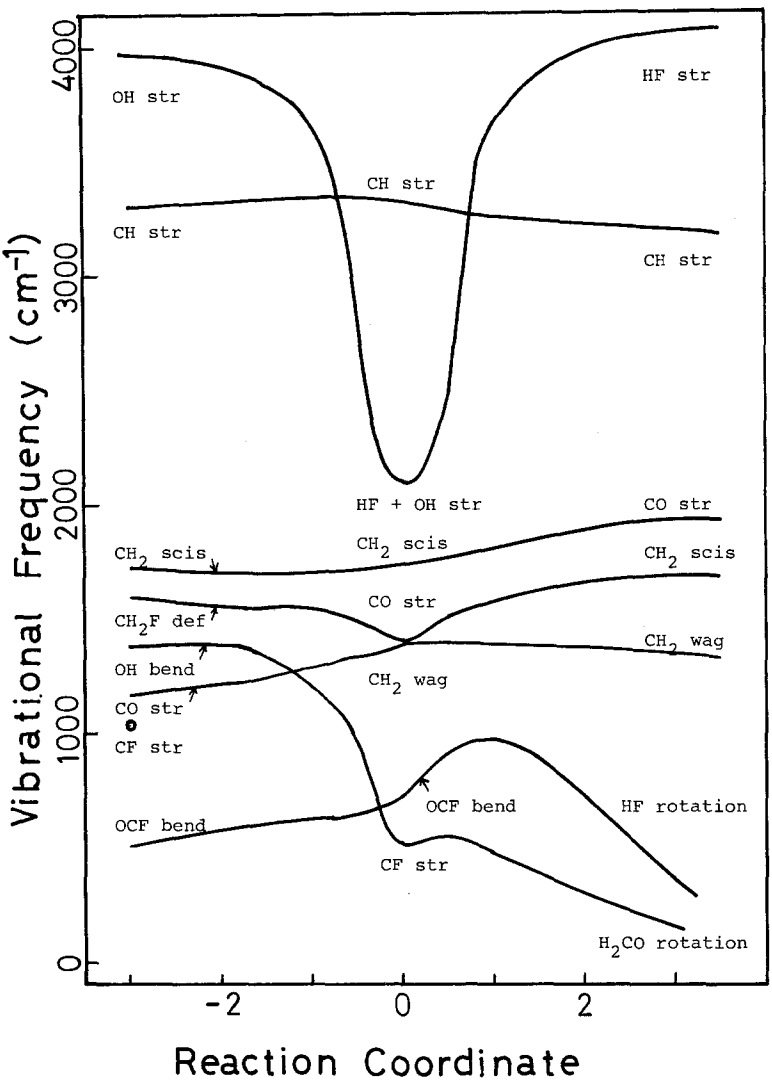

Fig. 6. Vibrational frequency correlation diagram of the HF elimination

diagonalyzing the projected force constant matrix [9, 10, 14, 19] where the degrees of freedom of IRC, overall translations and rotations are already projected out.

At first, we notice that there is no mode which correlates with the CF stretching mode at the reactant complex. This indicates that the IRC is parallel to this normal mode in the vicinity of the equilibrium point. Since the geometry of the transition state is a four-centered one, the stretching modes and the bending modes are complicatedly coupled with each other. The frequencies of the CH stretching,

CH_2 scissor, CH_2F deformation, and C=O stretching modes which correlate with the normal modes of the product H_2CO change moderately. The OH and OCF bending modes at the reactant complex can be utilized in the products relative rotational excitations. The most interesting product HF stretching mode is linked with the OH stretching mode of the reactant complex and furthermore both change their frequencies drastically in a narrow region caused by the interaction with the IRC. The IRC of HF elimination, therefore, twists in the configuration space coupled with the OH stretching mode immediately before the transition state, and just after surmounting the point coupled with the HF stretching mode. In analogy to the fact that the detection of a vibrationally excited HF stretching mode is related with the IRC twisting, the vibrational excitation of the OH stretching mode effectively promotes the reaction by application of microscopic reversibility.

The following conclusions can be drawn from the present calculations. If the HF elimination reaction proceeds in the complex mode, that is, some randomization occurs in the reactant complex, the coupling between the HF stretching mode and the IRC in the exit valley plays the central role in the vibrational excitation of HF. On the other hand, in case of the direct mode, the excitation of the OCF bending and OH stretching modes originated from the insertion mechanism are responsible for vibrational and rotational excitations of the HF molecules.

Acknowledgement. The authors are grateful to Dr. Kimihiko Hirao for the use of his direct CI program. The numerical calculations were carried out at the Data Processing Center of Kyoto University and at the Computer Center of IMS. Financial support was given by a Grant-in-Aid for Scientific Research from the Japanese Ministry of Education, Science and Culture.

References

1. For a recent review of reactions of O(^{1}D and ^{3}P), see Lin, M. C.: Adv. Chem. Phys. **62**, 113 (1980)
2. (a) Tully, J. C.: J. Chem. Phys. **61**, 61 (1974); **62**, 1893 (1975); (b) Walch, S. P., Dunning, T. H.: **72**, 3221 (1980)
3. Umstead, M. E., Woods, F. J., Lin, M. C.: J. Phys. Chem. **83**, 1289 (1979)
4. Burks, T. L., Lin, M. C.: Chem. Phys. **33**, 327 (1978)
5. Polanyi, J. C.: Acc. Chem. Res. **5**, 161 (1972)
6. Levine, R. D., Bernstein, R. B.: Molecular reaction dynamics. Oxford: Oxford Univ. Press 1974
7. Fukui, K.: J. Phys. Chem. **74**, 4161 (1970)
8. Kato, S., Kato, H., Fukui, K.: J. Am. Chem. Soc. **99**, 684 (1977)
9. Yamashita, K., Yamabe, T., Fukui, K.: Chem. Phys. Letters, **84**, 123 (1981)
10. Yamashita, K., Yamabe, T., Fukui, K.: J. Am. Chem. Soc. (in press)
11. Robinson, P. J., Holbrook, K. A.: Unimolecular reactions. New York: Wiley 1973
12. We used the HONDO program; Dupuis, M., King, H. F.: J. Chem. Phys. **68**, 3998 (1978)
13. Ditchifield, R., Hehre, W. J., Pople, J. A.: J. Chem. Phys. **54**, 724 (1971)
14. Kato, S., Morokuma, K.: J. Chem. Phys. **73**, 3900 (1980)
15. (a) We used the direct CI program by Dr. K. Hirao; (b) Roos, B. O., Siegbahn, P. E., in: Modern theoretical chemistry, Vol. 3, H. F. Schaefer, ed. New York: Plenum 1977
16. E. R. Davidson and D. W. Silver, Chem. Phys. Lett., **52**, 403 (1977)
17. Pulay, in "Modern Theoretical Chemistry", Vol. 3, H. F. Schaefer, ed. New York: Plenum. 1977

18. Kato, S., Fukui, K.: J. Am. Chem. Soc. **98**, 6395 (1976)
19. Miller, W. H., Handy, N. C., Adams, J. E.: J. Chem. Phys. **72**, 99 (1980); Gray, S. K., Miller, W. H., Yamaguchi, Y., Schaefer, H. F.: J. Chem. Phys. **73**, 2733 (1980)

Received November 4, 1981